Mineralocorticoid *versus* Glucocorticoid Receptor Occupancy Mediating Aldosterone-Stimulated Sodium Transport in a Novel Renal Cell Line

Hans-Peter Gaeggeler, Elena Gonzalez-Rodriguez, Nicole Fowler Jaeger, Dominique Loffing-Cueni, Rikke Norregaard, Johannes Loffing, Jean-Daniel Horisberger, and Bernard C. Rossier

Department of Pharmacology and Toxicology, University of Lausanne, Lausanne, Switzerland

Aldosterone controls sodium balance by regulating an epithelial sodium channel (ENaC)-mediated sodium transport along the aldosterone-sensitive distal nephron, which expresses both mineralocorticoid (MR) and glucocorticoid receptors (GR). Mineralocorticoid specificity is ensured by 11β-hydroxysteroid dehydrogenase type 2, which metabolizes cortisol or corticosterone into inactive metabolites that are unable to bind MR and/or GR. The fractional occupancy of MR and GR by aldosterone mediating the sodium transport response in the aldosterone-sensitive distal nephron cannot be studied *in vivo*. For answering this question, a novel mouse cortical collecting duct cell line ($mCCD_{cl1}$), which expresses significant levels of MR and GR and a robust aldosterone sodium transport response, was used. Aldosterone elicited a biphasic response: Low doses ($K_{1/2}$ = approximately 0.5 nM) induced a transient and early increase of sodium transport (peaking at 3 h), whereas high doses ($K_{1/2}$ = approximately 90 nM) entailed an approximately threefold larger, long-lasting response. At 3 h, the corticosterone dose-response curve was shifted to the right compared with that of aldosterone by more than two log concentrations, an effect that was fully reverted in the presence of the 11β-hydroxysteroid dehydrogenase type 2 inhibitor carbenoxolone. Low doses of dexamethasone (0.1 to 1 nM) failed to induce an early response, but high doses elicited a long-lasting response ($K_{1/2}$ = approximately 8 nM), similar to that observed for high aldosterone concentrations. Equilibrium binding assays showed that both aldosterone and corticosterone bind to a high-affinity, low-capacity site, whereas dexamethasone binds to one site. Within the physiologic range of aldosterone concentrations, sodium transport is predicted to be controlled by MR occupancy during circadian cycles and by MR and GR occupancy during salt restriction or acute stress.

J Am Soc Nephrol 16: 878-891, 2005. doi: 10.1681/ASN.2004121110

Transepithelial Na^+ and K^+ transports are regulated by mineralocorticoid hormones in the aldosterone-sensitive distal nephron (ASDN), in the distal colon, and in other epithelia characterized by a high transmural electrical resistance ("tight" epithelia) and an amiloride-sensitive, electrogenic sodium transport (1). The resulting changes in urinary Na^+ and K^+ excretion are responsible for the regulation of the sodium and potassium balance of the organism. *In vivo*, the early effect of aldosterone was observed in adrenalectomized rats with a latent period of approximately 30 min and was fully inhibited by Actinomycin D (2,3). The genomic action of aldosterone is a three-step mechanism: (*1*) binding to its cognate receptor followed by its translocation into the nucleus; (*2*) binding of the liganded receptor to hormonal regulatory elements situated on the promoter of a selected number of genes, leading to transcription activation or repression (aldosterone induced-[AIT] or -repressed transcripts [ART]); and (*3*) translation into their respective aldosterone-induced (AIP) or -repressed proteins (ARP) mediating in turn the upregulation of amiloride-sensitive electrogenic sodium transport (1).

In its target cell, aldosterone is known to bind to two types of binding sites (4): a high-affinity, type 1 binding site (K_d = approximately 0.5 to 2 nmol/L), and a low-affinity (K_d = approximately 14 to 60 nmol/L), type 2 binding site (5–7), which have been tentatively identified with the proteins known as the mineralocorticoid (MR) and glucocorticoid (GR) receptors, respectively. Corticosterone (or cortisol) binds with the same affinity as aldosterone to type 1 binding site and a higher affinity to type 2 binding site. Dexamethasone has a high affinity for type 2 binding site and a lower affinity for type 1. In an earlier work in the toad bladder system, we established a quantitative correlation between occupancy of type 1 (MR) *versus* type 2 (GR) receptor, with the early *versus* late response to aldosterone (8). We concluded that occupancy of both type 1 (MR) and type 2 (GR) was necessary to achieve maximal sodium transport across this tight epithelia. Occupancy of type 1 receptor was related mainly to the early phase of aldosterone action, whereas the late response correlated with occupancy of type 2 receptor. The limitations of the toad bladder system were

Received December 21, 2004. Accepted January 22, 2005.

Published online ahead of print. Publication date available at www.jasn.org.

Address correspondence to: Dr. Bernard C. Rossier, Département de pharmacologie et de toxicologie, Université de Lausanne, Rue du Bugnon 27, CH-1005 Lausanne, Switzerland. Phone: +4121-692-5351; Fax: +4121-692-5355; E-mail: Bernard.Rossier@unil.ch

ISSN: 1046-6673/1604-0878

significant: (*1*) a detailed dose-response curve could not be technically achieved, (*2*) the effects of glucocorticoid agonist or antagonist were not studied, (*3*) the relevance of the amphibian model to the function of the mammalian cortical collecting duct was uncertain, and (*4*) the 11β-hydroxysteroid dehydrogenase type 2 (11β-HSD2) mechanism was not yet known. Mineralocorticoid specificity is indeed achieved by the presence of 11β-HSD2, an enzyme that metabolizes cortisol into cortisone (or corticosterone into 11β-dehydrocorticosterone) with only 0.3% affinity to MR receptor (9,10). The enzyme has a high V_{max} in cortical collecting duct (CCD) cells so that the MR should be protected from illicit occupation by free plasma cortisol (or corticosterone), which may circulate at >100-fold excess over aldosterone in the plasma. The model predicts that GR could be occupied by aldosterone, but the physiologic relevance of this binding for mediating the sodium transport response is not known. To address this question and to study the respective role of aldosterone and glucocorticoids as well as their cognate receptors for sodium transport by the ASDN, we took advantage of a novel spontaneously transformed cell line derived from CCD primary cultures. Our principal aims were to establish (*1*) a quantitative correlation of MR *versus* GR occupancy with the sodium transport response for agonist (aldosterone, corticosterone, and dexamethasone) and in the presence of MR antagonist (spironolactone) or GR antagonist (RU486) and (*2*) the role of the 11β-HSD2 in the protection of MR *in vitro.* This enabled us to correlate the physiologic variations of plasma corticosteroid in function of the circadian rhythm and the salt intake and their pathophysiologic variations during stress and hypovolemia, with the predicted occupancy of MR or GR.

Materials and Methods

Materials

DMEM/Ham's F_{12} (1:1 vol/vol) was from Life Technologies Invitrogen (Switzerland). (^{3}H)corticosterone, (^{3}H)aldosterone, and (^{3}H)dexamethasone were from Amersham Bioscience (Otelfingen, Switzerland). Hormones and reagents were from Sigma (St. Louis, MO). Spironolactone and RU 486 were 10 mM stock solution in 100% ethanol. Aldosterone was 10 mM stock solution in 100% DMSO. Stock solutions are diluted to their final concentrations in DMEM. FCS was from Fisher Scientific (Wohlen, Switzerland). FCS was always selected after growth and electrophysiologic screening (responses to aldosterone and vaso-

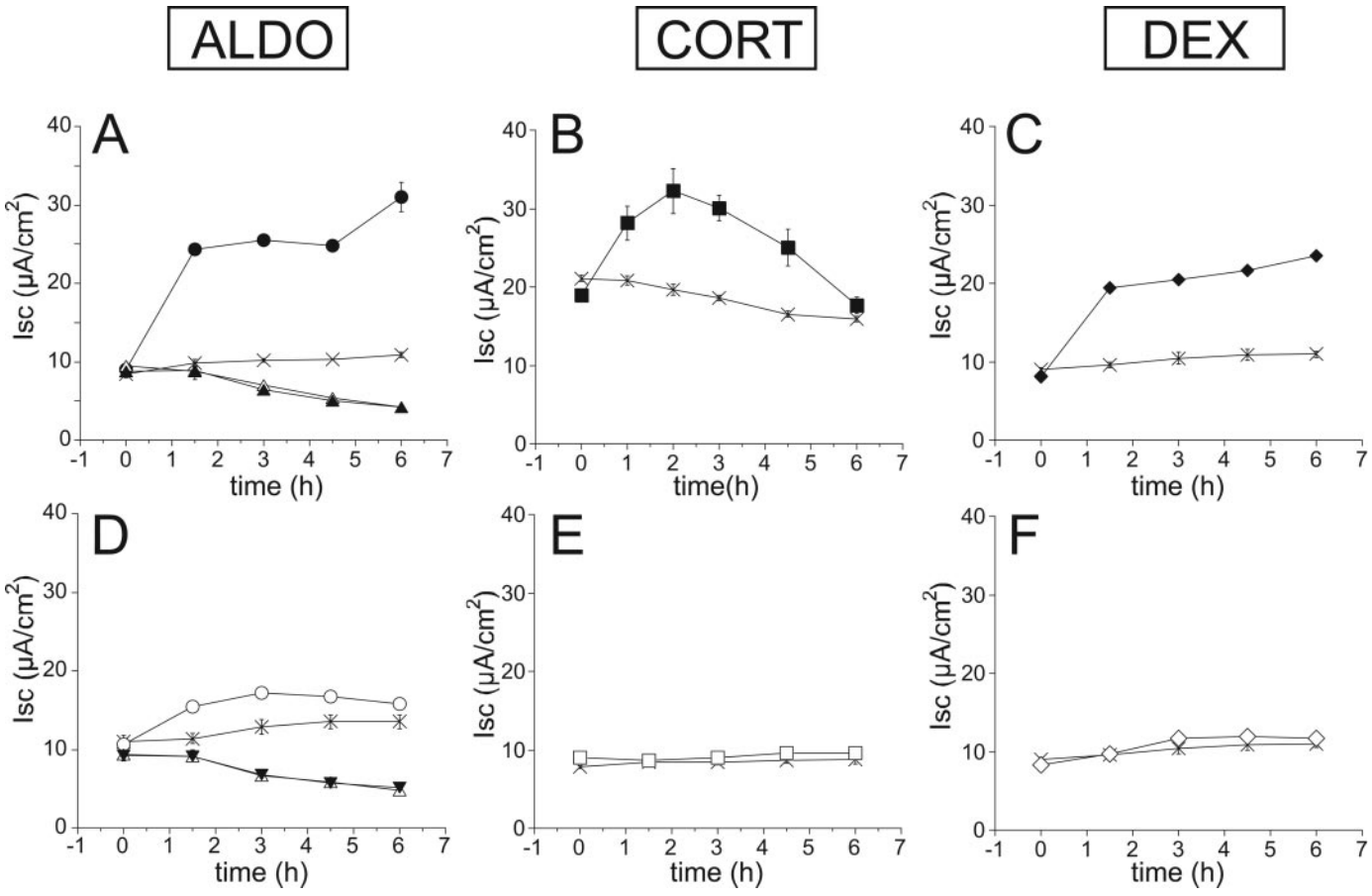

Figure 1. General features of the sodium transport response to corticosteroids in $mCCD_{cl1}$ cells. (Left) Time-dependent effect of aldosterone on short-circuit current (I_{sc}). (A) Aldosterone 300 nM (●) *versus* Control (X) *versus* Act D (△) *versus* Act D + aldosterone (▲). (D) Aldosterone 0.3 nM (○) *versus* Control (X) *versus* Act D (△) *versus* Act D + aldosterone (▲). (Middle) Time-dependent effect of corticosterone on I_{sc}. (B) Corticosterone 300 nM (■) *versus* Control (X). (E) Corticosterone 0.3 nM (□) *versus* Control (X). (Right) Time-dependent effect of corticosterone on I_{sc}. (C) Dexamethasone 300 nM (♦) *versus* Control (X). (F) Dexamethasone 0.3 nM (◇) *versus* Control (X).

pressin) of eight to 10 different batches of sera provided by different companies. Only approximately 20% of the sera tested were found to be able to sustain growth and full differentiation. Tissue Culture treated Transwell (0.4 μM pore size, 4.5 cm^2 diameter) were from Corning Costar Corp. (Cambridge, MA). Collagen was prepared from rat tails kept in 70% ethanol. Fibers were dissected from dried tails, and wet was weight determined (10 tails yield approximately 5 g of wet collagen). Collagen was solubilized in acetic acid (1/1000 vol/vol) by gentle stirring for 24 h at 4°C and at a concentration of 5 g (wet wt) collagen/L. The collagen solution was heated up to 36°C, prefiltered, and then filtered through a Millipore apparatus under pressure (90 mm filter/7 kg per cm^2) using progressively smaller pore size down to 0.2 μM. Filter cups (Transwell Costar 3412 [4.7 cm^2] or 3119 [44 cm^2]) were coated by adding 0.5 ml (or 3 ml, respectively) of collagen solution, and excess solution was removed until a thin layer of approximately 10 $\mu l/cm^2$ was obtained. Collagen then was polymerized for 24 h at room temperature adding 250 μl of NH_3 (28%) in empty spaces between wells. After NH_3 was removed, filters were preincubated with growth medium (1.5 ml apical and 2.5 ml basolateral) for 24 h, and seeding was performed using fresh medium.

Culture Media

Growth medium was DMEM supplemented with insulin (0.87 μM), human apotransferrin (5 μg/ml), EGF (10 ng/ml), T3 (1 nM) dexamethasone (50 nM), penicillin (100 μ/ml), streptomycin (130 μg/ml), and 2% FCS. Filter cup medium was DMEM supplemented with 3 nM dexamethasone.

Establishment of the $mCCD_{cl1}$ Cell Line

The generation of the Liddle mice has been described previously (11). For *in vitro* primary cell culture experiments, L/L, L/+, and +/+ littermates were used. Confluent primary cultures of CCD microdissected from kidney βENaC +/+, L/+, and L/L mice were grown in growth medium, according to the previously described method (12,13). More than 60 primary cultures from each genotype were dissociated in EDTA trypsin solution and seeded on 96-tissue culture dishes. Cells were passaged every other week, and a number of single clones that spontaneously went on dividing beyond five passages could be isolated from either genotype. In the present article, we describe one clone of wild-type origin that we term $mCCD_{cl1}$.

Electrophysiologic Studies

Confluent cells that were seeded and grown in growth medium on collagen-coated Transwells for 5 d then were grown for another 5 d in filter cup medium and then overnight in DMEM before measuring sodium transport response to steroid hormones. Short-circuit current (I_{sc} in $\mu A/cm^2$) was measured by clamping transepithelial potential difference (P_D in mV) to 0 for 10 s, and transepithelial electrical resistance (Ohm/cm^2) was recorded under sterile condition using a homemade voltage clamp apparatus. Each batch of rat-tail collagen was screened for its ability to confer high transepithelial electrical resistance (>4000 Ohm/cm^2) and hormone responsiveness. Kinetic parameters (half-activation constant [$K_{1/2}$] and maximal I_{sc} [I_{scmax}]) for one- or two-site models were calculated using the nonlinear fit routine of the Kaleidagraph program (Synergy Software, Reading, PA).

Corticosteroid Binding Assay

$mCCD_{cl1}$ were grown until confluence in 100-mm Petri dishes (7 d), incubated for 2 h in a Ringer solution (143 mM NaCl, 17.5 mM $NaHCO_3$, 4 mM KCl, 0.8 mM KH_2PO_4, 10 mM glucose, 1 mM and $CaCl_2$), then rinsed in fresh Ringer solution for another 2 h and then gently scraped off the dishes, centrifuged for 5 min at 150 × *g*, and the pellet snap-frozen in liquid nitrogen. The cells were homogenized by grinding them under liquid nitrogen. The powder was diluted threefold with buffer (220 mM sucrose, 10 mM TES, 12 mM Thioglycerol, 25 mM KCl, and 1.5 mM EDTA adjusted to a pH of 7.0), complemented with 1 mM dithiothreitol, then centrifuged for 7 min at 48,000 × *g*. Cell cytosol preparations were complemented with 10 mM Na-Molybdate and immediately used for steroid binding assays (14) or frozen in liquid nitrogen for further use. Aliquots of cytosol (130 μl) were incubated with 0.1 to 670 nM (^{3}H)aldosterone, (^{3}H)corticosterone, or (^{3}H)dexamethasone for 4 h at 4°C. Bound and free hormones were separated, using the dextran-charcoal method, and bound hormone was analyzed as a function of free hormone, using the Ligand software for fitting one or two binding-sites ± nonspecific binding. In a separate experiment, corticosteroid binding assay was performed on cells that had been grown on large Costar Transwell (50 cm^2) and grown until development of a basal sodium transport and a high transepithelial electrical resistance (5 to 10 $\mu M/cm^2$ and up to 8000 Ohm/cm^2).

Table 1. Summary of electrophysiologic data[a]

Time (H)	Control			Aldosterone 0.3 nM			Aldosterone 300 nM		
	I_{sc}	P_D	R	I_{sc}	P_D	R	I_{sc}	P_D	R
t_0	7.65	27.0	3518	7.92	28.7	3591	8.05	30.7	3825
±SD	1.85	11.3	886	2.27	13.7	1047	2.16	16.2	1532
$t_{3\ h}$	10.00	27.9	3011	14.3	39.0	2864	28.6	64.0	2377
±SD	3.16	12.6	1183	2.4	19.0	1372	5.3	20.7	1244
$t_{24\ h}$	5.73	20.1	3760	6.1	26.4	4215	20.2	51.8	3058
±SD	2.43	8.7	1131	1.8	11.2	1100	8.0	14.7	982
n		11			9			9	
		(27)			(21)			(21)	

[a] I_{sc} ($\mu A/cm^2$) P_D (mV) R (ohm/cm^2) are mean ± SD; *n* = number of experiments (number of filters). The variability of the measurement was low between duplicate or triplicate within one experiment, so values of duplicate or triplicate filters were used throughout the whole study. The variability between experiments was also low and the reproducibility was satisfactory, so direct comparisons between experiments were possible.

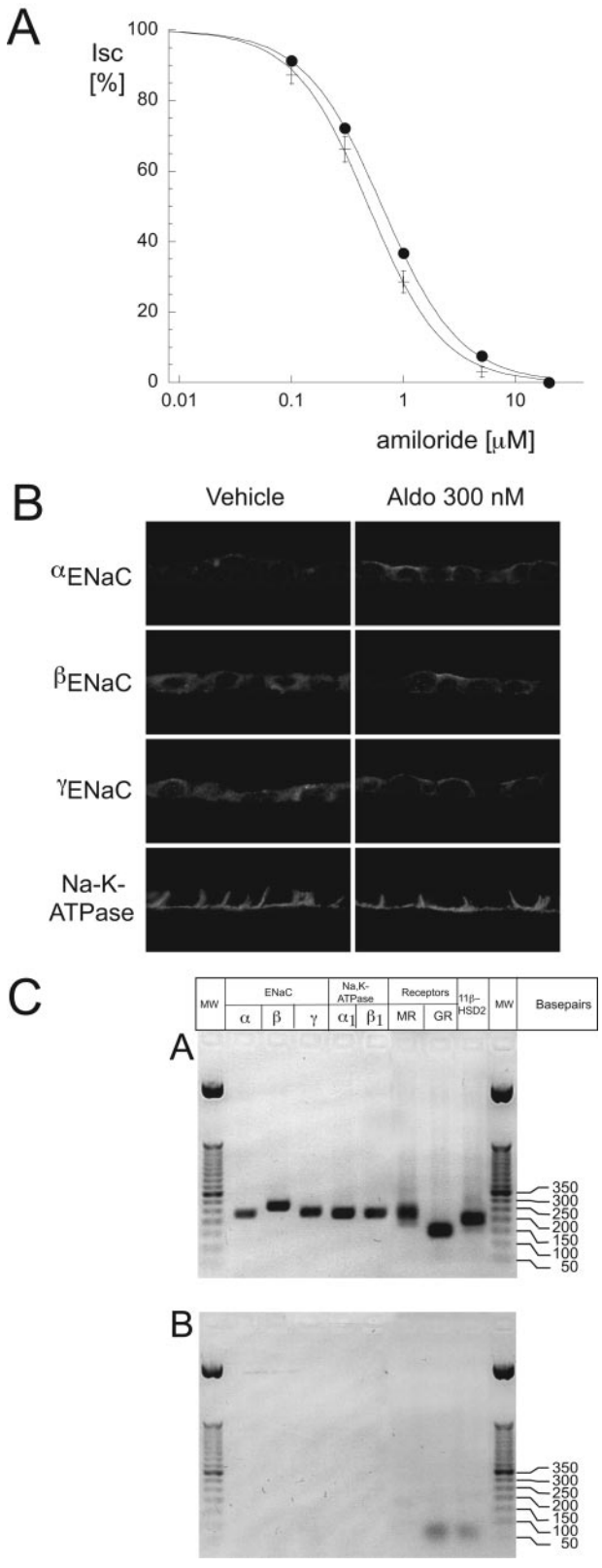

Figure 2. Epithelial polarity of $mCCD_{cl1}$ cells grown on filter cups. (A) Dose-response curve of amiloride on I_{sc}. Aldo (300 nM; ●) *versus* Control (+) at 3 h. Results are expressed as % of $\Delta I_{sc} = I_{sc}$ measured in the absence of amiloride $- I_{sc}$ measured at maximal concentration of amiloride. I_{sc} baseline currents were 10 μA (control) and 185 μA (aldo; $n = 6$ filters). (B) Immunolocalization of α, β, and γ epithelial sodium channel (ENaC) and Na,K-ATPase (β subunit). $mCCD_{cl1}$ cells grown on filters in the absence of hormone (left, control) or in the presence of aldosterone (300 nM, 3 h; right, aldo). (C) Detection by reverse transcription–PCR (RT-PCR) of glucocorticoid receptor (GR), mineralocorticoid receptor (MR), 11β-hydroxysteroid dehydrogenase type 2 (11β-HSD2), ENaC, and Na,K-ATPase transcripts in control cells.

Immunofluorescence

Cells that were grown on permeable support were prepared for immunofluorescence, as described previously (15). The epithelial sodium channel (ENaC) (16) and Na-K-ATPase (17) antibodies were previously described. Cells were fixed with 3% paraformaldehyde in PBS for 15 min, rinsed twice with PBS, embedded in "Neg-50" frozen section medium (Richard Allen Scientific, Kalamazoo, MI), frozen in propane that was liquefied by liquid nitrogen, and sectioned perpendicular to the underlying filter membrane in a cryostat. Sections (5 μm thick) were placed on chrome alum gelatin-coated glass slides, preincubated with 10% normal goat serum in PBS, and incubated overnight at 4°C with rabbit antibodies against rat αENaC (dilution 1:500), rat βENaC (dilution 1:1000), rat γENaC (dilution 1:400), or rat α subunit of Na-K-ATPase (dilution 1:8000). Binding sites of the primary antibodies were detected with Cy3-conjugated goat anti-rabbit IgG (Jackson ImmunoResearch Laboratories, West Grove, PA). For control of unspecific binding of primary or secondary antibodies, we performed incubations with nonimmune sera or by omitting the primary antibody. All control experiments were negative. Sections were mounted in Dako glycergel (Dako, Glostrup, Denmark), to which 2.5% 1,4-diazobicyclo(2,2,2)octane (DABCO; Sigma) was added as fading retardant. Sections were analyzed by epifluorescence with a Zeiss microscope, and images were acquired with a charge-coupled device camera.

Detection of mRNA

For reverse transcription–PCR, $mCCD_{cl1}$ cells that ere grown in filter were lysed and homogenized (QIAshredder; Qiagen, Studio City, CA), and total RNA was extracted (RNeasy Mini Kit; Qiagen). A total of 250 ng of reverse-transcribed total RNA at 37°C for 1 h using the Superscript II (Invitrogen) was amplified by PCR. The same quantity of reverse transcription mix in the absence of the enzyme was used as a negative control. ENaC and Na,K-ATPase subunit cDNA were amplified for 30 cycles in 50 μl of total volume that contained 2.5 U of TaqDNA Polymerase (Amersham Biosciences) and 10 pmol of specific primers. Annealing temperature was 58°C. The primers used were αENaC 5′-CGGAGTTGCTAAACTCAACATC-3′ (sense) and 5′-TGGAGACCAGTACCGGCT-3′ (antisense), βENaC 5′-ATGTGGTTCCTGCTTACGCTG-3′ (sense) and 5′-GTCCTGGTGGTGTTGCTGTG-3′ (antisense), γENaC 5′-CCAAAGCCAGCAAATAAACAAA-3′ (sense) and 5′-GCGGCGGGCAATAATAGAGA-3′ (antisense), Na,K-ATPase α1 5′-CCATCGCTTACACCCT-3′ (sense) and 5′-CAGACGCTCGTTCACA-3′ (antisense), and Na,K-ATPase β1 5′-GCCCCTAAGTATTGCCG-3′ (sense) and 5′-TGGGCCGTTACCTTTG-3′ (antisense). MR, GR, and 11β-HSD_2 cDNA were amplified using the QuantiTect SYBR Green PCR kit (Roche) as recommended by the manufacturer. Amplification was done on a LightCycler (Roche), and cDNA were amplified for 60 cycles in 20 μl of total volume; annealing temperature was 55°C. The primers used were MR 5′-ATAGAGGCTCAAGGTCACAC-3′ (sense) and 5′-GAGAAGAACGCTCCAAGGTC-3′ (antisense), GR 5′-GGGCTATGAACTTCGCAG-3′ (sense) and 5′-CATCGGAGCACACCAG-3′ (antisense), and 11β-HSD2 5′-ACTGCGTGACCTCTGT-3′ (sense) and 5′-CTTGCGGAAAGTCGCC-3′ (antisense).

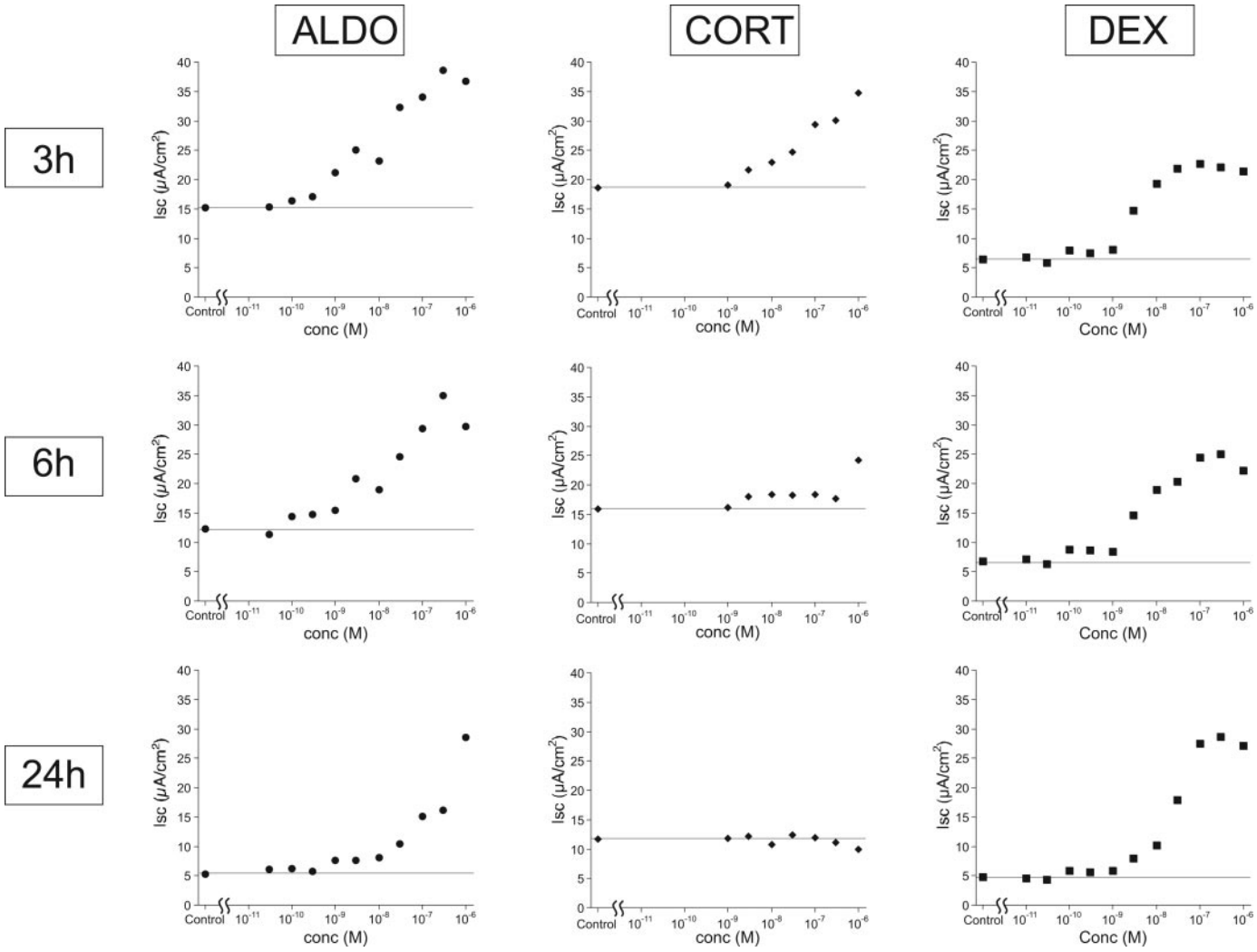

Figure 3. Dose-response curves for mineralo- and glucocorticoid agonists aldosterone, corticosterone, and dexamethasone. Dose-response curve for Aldo (●), Cort (♦) and Dex (■). (Left) Aldo top 3 h, middle 6 h, bottom 24 h. (Middle) Cort top 3 h, middle 6 h, bottom 24 h. (Right) Dex top 3 h, middle 6 h, bottom 24 h. The horizontal line represents the values of basal I_{sc} in the absence of hormones.

Table 2. Summary of electrophysiologic data: $K_{1/2}$ for aldosterone, corticosterone, and dexamethasone at 3, 6, and 24 h

Time	Aldosterone $K_{1/2}$ (nM)		Corticosterone $K_{1/2}$ (nM)	Dexamethasone $K_{1/2}$ (nM)
	High Affinity	Low Affinity		
$t_{3\ h}$	0.52[a]	89	18.2	9.7
$t_{6\ h}$	0.50[a]	95	161	20
$t_{24\ h}$	0.65	ND	ND	ND
Best fit two- *versus* one-site model	$P<0.001$		NS	NS

[a]Two-site model fit data better than one-site model, $P = 0.005$, extra sum-of-square F test. ND, not determined.

Amplification products were run on a 2% agarose gel, stained with ethidium bromide, and photographed. For RT-PCR, $mCCD_{cl1}$ cells that were grown on filters were lysed and homogenized. (A) PCR on total RNA reverse-transcribed on cDNA using the Superscript II (Invitrogen). (B) PCR on total RNA when the reverse transcriptase Superscript II was not added to the reverse-transcription mix. Lanes in B correspond to those of A. The PCR products name and the sizes of the DNA ladder are indicated in the figure. The expected sizes are αENaC, 229 bp; βENaC, 265 bp; γENaC, 228 bp; Na,K-ATPase α1, 224 bp; Na,K ATPase β1, 222 bp; MR, 226 bp; GR, 141 bp; and 11β-HSD_2, 193 bp.

Statistical Analyses

Results are given as means ± SEM for n experiments. Statistical differences between groups were calculated using t test.

Results

General Features of the Sodium Transport Response in $mCCD_{cl1}$ Cells

As shown in Figure 1, the $mCCD_{cl1}$ cells had a baseline short-circuit current at approximately 10 μAmps/cm^2, which remained stable over a 6-h incubation. Upon maximal stimulation by aldosterone (300 nM; Figure 1A), the short-circuit current increased rapidly to reach maximal value after 5 to 6 h (>30 μAmps/cm^2). In the presence of actinomycin D (2 μg/ml), the aldosterone response was fully inhibited and indistinguishable from the actinomycin D–treated control cells. At 6 h, actinomycin D had no obvious cytotoxic effect; transepithelial resistances (data not shown) were maintained above baseline values (ActD [>6000 Ohm/cm^2] *versus* ActD+Aldo [>6000 Ohm/cm^2] *versus* control [>4000 Ohm/cm^2] *versus* Aldo [>2000 Ohm/cm^2]). Upon stimulation of a low dose of aldosterone (0.3 nM; Figure 1D), the sodium transport peaked at 3 h, reaching approximately 35% of the response observed at 300 nM aldosterone, and then progressively declined to control levels. Actinomycin D fully inhibited the response. These data indicate that the aldosterone response is critically dependent on the genomic action of aldosterone, as it has been shown in a variety of experimental models *in vivo* (18) and *in vitro* (see review in (1)). As shown above in Figure 1, A and D, the pattern of aldosterone response differs dramatically at low (0.3 nM; Figure 1D) *versus* supramaximal concentrations (300 nM; Figure 1A). As shown in Figure 1, B and E, the pattern of corticosterone response is also time and dose dependent. At 300 nM corticosterone (Figure 1B), the sodium transport response peaked at 3 h and then decreased progressively toward baseline controls. At 0.3 nM corticosterone (Figure 1E), there was no significant sodium transport response at any time. As shown in Figure 1, C and F, the pattern of dexamethasone response is different from that of aldosterone or corticosterone. At 300 nM dexamethasone (Figure 1C), the sodium transport response peaked at 6 h and remained at almost the same level for the next 21 h. At 0.3 nM dexamethasone (Figure 1F), there was no significant sodium transport response at any given time. Table 1 summarizes the P_D, I_{sc}, and R values of all experiments performed in the course of this study at low (0.3 nM) *versus* high (300 nM) aldosterone concentration. The $mCCD_{cl1}$ cells have been so far passaged, up to 40 times. The aldosterone responsiveness was maintained at high passage numbers. The early response at low aldosterone concentrations was consistently between 20 and 35% of the maximal response observed at 300 nM. Experiments of the present study were performed on cells from p19 to p33.

The observed electrogenic sodium transport was amiloride sensitive (Figure 2A). Increasing concentrations of amiloride from 0.01 to 10 μM progressively and fully inhibited both the baseline- and the aldosterone-stimulated sodium transport. In the presence of 140 mM sodium, the Ki for amiloride was 650 nM, not statistically different from the inhibition of aldosterone-stimulated so-

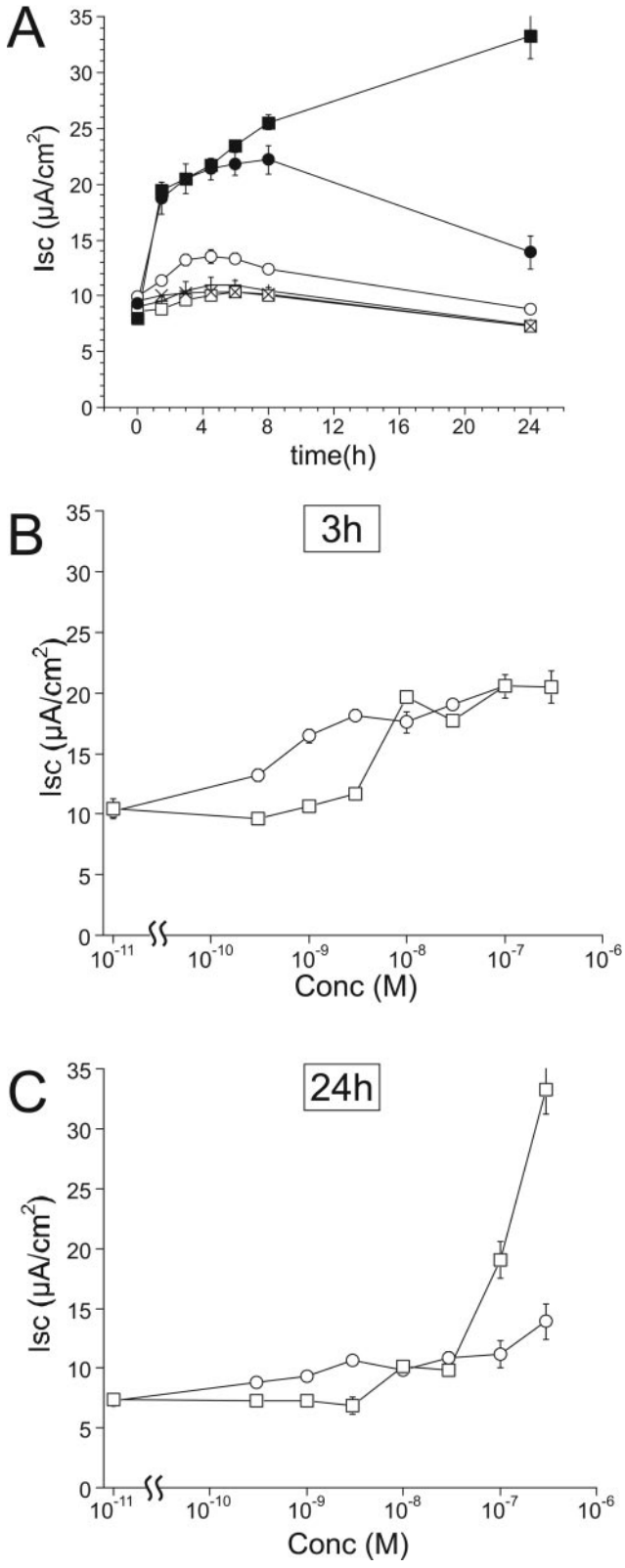

Figure 4. Differential effects of aldosterone *versus* dexamethasone on I_{sc}. (A) Time course of Aldo 300 nM (●) *versus* 0.3 nM (○) *versus* Dex 300 nM (■) *versus* 0.3 nM (□) *versus* control (X). (B) Dose-response curve Aldo (○) *versus* Dex (□) at t 3 h. (C) Dose-response curve Aldo (○) *versus* Dex (□) at 24 h

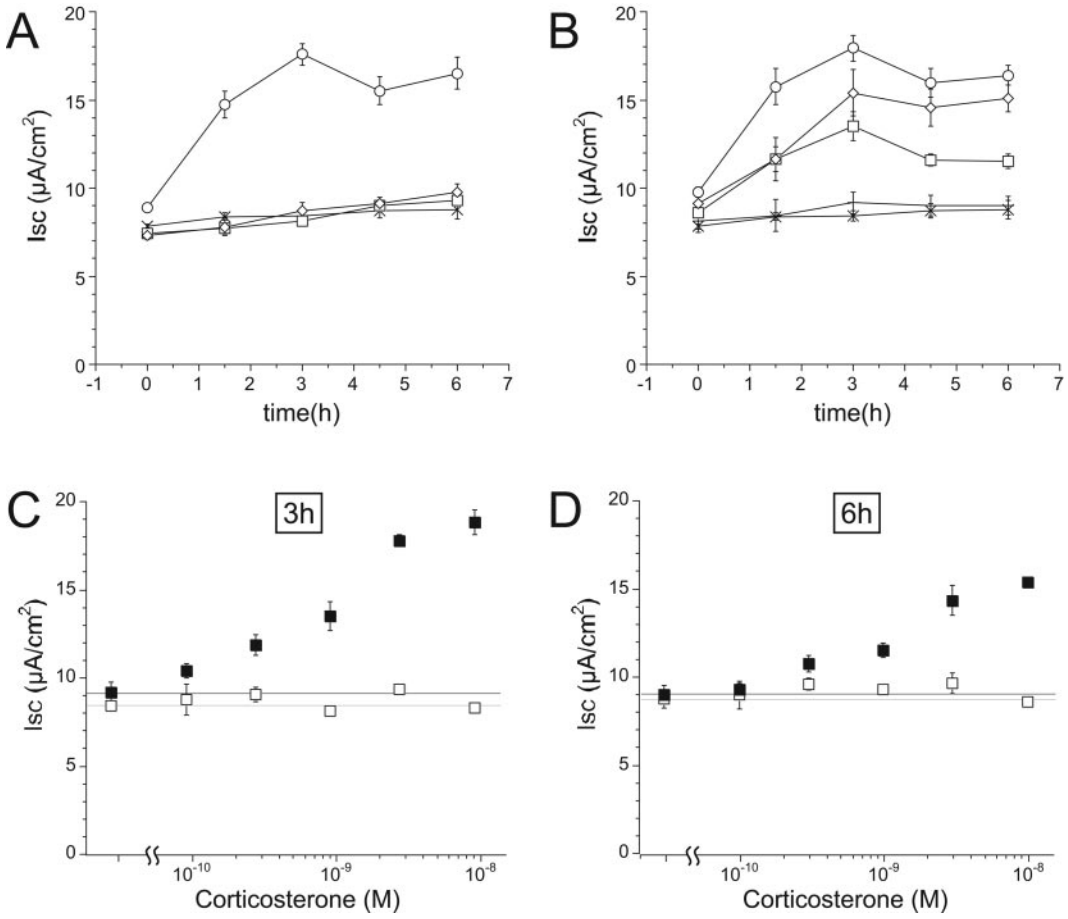

Figure 5. Evidence for protection of MR/GR by inhibition of 11β-HSD2 by carbenoxolone. Effect of carbenoxolone (Cbx) on the corticosterone, aldosterone, and dexamethasone dose-response curves. (A) Time course of Aldo (1 nM; ○) *versus* Cort (1 nM; ◇) *versus* Dex (1 nM; □) *versus* control/diluent without Cbx (X). (B) Time course of Aldo (1 nM; ○) *versus* Cort (1 nM; ◇) *versus* Dex (1 nM; □) all with Cbx *versus* Cbx (10 μM; +) *versus* control/diluent (X). (C) Dose-response of Cort in the absence of Cbx (□) or presence of Cbx (10 mM; ■). (D) Dose-response of Cort in the absence of Cbx (□) or presence of Cbx (10 μM; ■) at 6 h.

dium transport (Ki = 490 nM). This sensitivity to amiloride is consistent with an ENaC-mediated sodium transport.

In the CCD, the electrogenic amiloride-sensitive sodium transport is mediated by ENaC localized at the apical membrane and Na,K-ATPase localized at the basolateral membrane. As shown in Figure 2B, aldosterone (300 nM, 3 h) elicited an increased localization of α, β, and γ ENaC subunits at the apical membrane of the cells, whereas the Na,K-ATPase decorated the basolateral membrane and was not influenced by aldosterone treatment. Reverse transcription–PCR revealed that $mCCD_{cl1}$ cells express not only ENaC and Na,K-ATPase but also MR, GR, and 11β-HSD2 (Figure 2C).

Dose-Response Curves for Mineralo- and Glucocorticoid Agonists Aldosterone, Corticosterone, and Dexamethasone

Next, dose-response curves for the three agonists (aldosterone, corticosterone, and dexamethasone) were performed over a large range of concentrations (0.01 to 300 nM) to cover the full range of receptor occupancy by the two ligands on MR or GR. As shown in Figure 3, ALDO left, the dose-response curve varies depending on the time of exposure to aldosterone. At 3 h and 6 h, the dose-response (Figure 3, top and middle left) is biphasic. As shown in Table 2, two $K_{1/2}$ can be derived from the data: The first at 0.5 nM and the second one at 89 nM. At 24 h (Figure 3, ALDO bottom left, and Table 2), the response elicited by low dose of aldosterone had greatly diminished ($K_{1/2}$ = approximately 0.65 nM) or vanished (see Figure 1A); the remainder of the response was characterized by a $K_{1/2}$ that progressively shifted to the right: 95 nM (6 h) and over (not determined) at 24 h.

As shown in Figure 3 (CORT top, and Table 2), at 3 h, corticosterone induced a sodium response that was significantly shifted to the right with at least 40-fold less potency ($K_{1/2}$ = approximately 18 nM). At 6 h, the responses to corticosterone were small ($K_{1/2}$ = approximately 160 nM) and became NS with respect to controls at 24 h (Figure 3, CORT middle and bottom). As shown below, this is likely to be due to the presence of 11β-HSD2, which is able to metabolize corticosterone (which binds with high affinity to both MR and GR) to 11β-dehydrocorticosterone, which has a very low affinity for either MR or GR.

As shown in Figure 3 (DEX top, and Table 2), at 3 h, the dose-response curve to the potent glucocorticoid agonist dexamethasone was monophasic with a $K_{1/2}$ of 10 nM, which shifted to the right after 6 h ($K_{1/2}$ = approximately 20 nM; Figure 3, DEX middle) and even more so after 24 h (Figure 3, DEX bottom) of incubation ($K_{1/2}$ >300 nM). This is also likely to be due to dexamethasone metabolism (see below). The cell line does respond to low concentrations of aldosterone, whereas dexamethasone has no effect. To confirm this observation, we performed an additional experiment in which we compared the dose-response curve for aldosterone and dexamethasone in the same set of dishes. As shown in Figure 4A, the expected effect of low *versus* high doses of aldosterone or dexamethasone were observed over a 24-h incubation. The difference of the dose-response curves for the two agonists is evident during the early phase (3 h) of aldosterone action (Figure 4B). The difference disappeared in a time-dependent manner, and after a 24-h incubation, dexamethasone became an even more potent agonist than aldosterone (Figure 4C).

Evidence for Protection of MR by 11β-HSD2

As shown in Figure 5A, corticosterone or dexamethasone alone (1 nM) had no detectable effect on sodium transport over a 6-h incubation, whereas aldosterone (1 nM) elicited a robust response. As shown in Figure 5B, carbenoxolone (10 μM), a potent inhibitor of 11β-HSD2, did not decrease baseline sodium transport. In the presence of carbenoxolone, corticosterone (and to some extent dexamethasone) induced a sodium transport response that was indistinguishable from that of aldosterone. As shown in Figure 5, C (3 h) and D (6 h), in the presence of carbenoxolone, corticosterone elicited a sodium transport response with a $K_{1/2}$ similar to that of aldosterone alone (see Figure 4A). Overall, the $mCCD_{cl1}$ cell seems to express all of the mechanisms described *in vivo* to confer mineralocorticoid specificity.

Mineralo- and Glucocorticoid Specificity of the Sodium Transport Response

The mineralocorticoid specificity was examined further by investigating the effect of spironolactone, an MR antagonist, and of RU 486, a GR antagonist, during the early phase of agonist action (3 h). As shown in Figure 6A, spironolactone alone had no effect on baseline sodium transport at concentrations below 10 μM. RU486 had no significant agonist activity, up to 30 μM (Figure 6B). In subsequent experiments, the concentration of spironolactone/RU486 was kept below 1 μM.

As shown in Figure 7A, a 100-fold excess of spironolactone fully inhibited the aldosterone response at 0.3, 1, 3, and 10 nM of aldosterone. By contrast, the aldosterone response within the same range of concentrations was not inhibited by a 100-fold excess of RU486 (Figure 7B). There was even a synergism (between 0.1 and 1 nM aldosterone) for which we have no explanation. The response to dexamethasone was not inhibited by spironolactone (Figure 7C) but was fully inhibited by RU486 (Figure 7D).

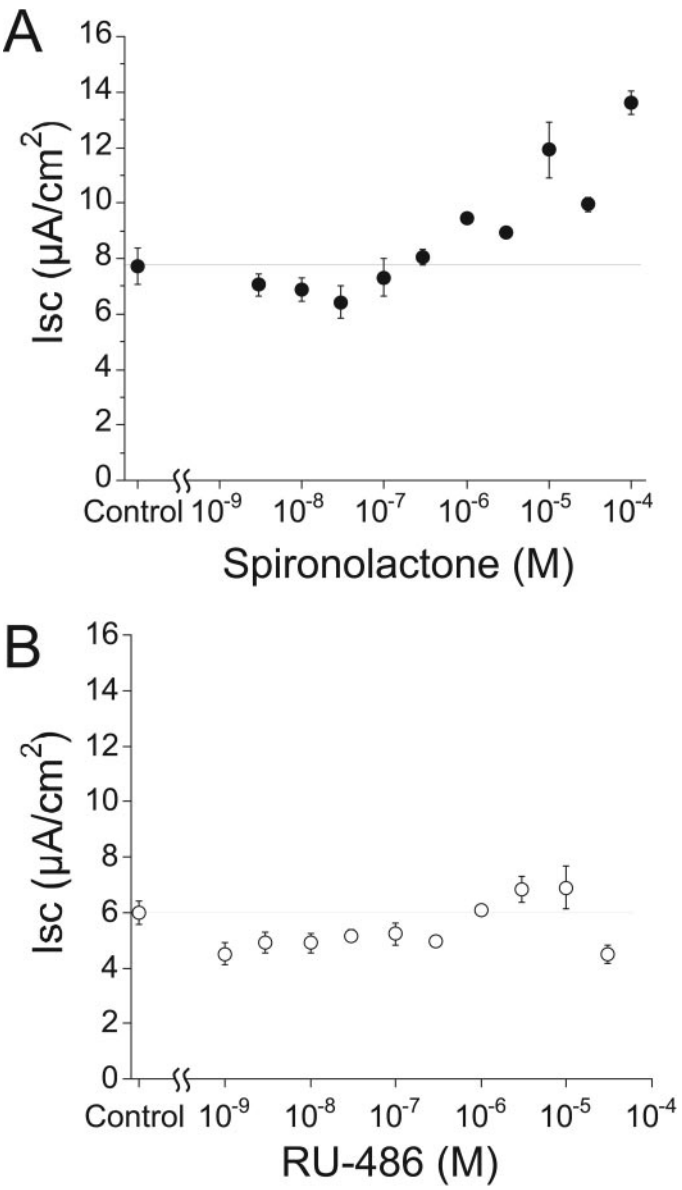

Figure 6. Effects of spironolactone and RU486 on baseline I_{sc}. (A) Dose-response curve (3 h) spironolactone (●). (B) Dose-response curve (3 h) RU486 (○). Baseline current in the absence of antagonist is indicated by the horizontal line.

Determination of MR and GR K_d and B_{max} for Aldosterone, Corticosterone, and Dexamethasone by Equilibrium Binding Assay

The affinity and the number of sites for the three agonists used in this study were determined by equilibrium binding assay on cytosol from cells that were grown either on plastic or on transwell filter cups, as described in the Materials and Methods section, and the data are displayed as Scatchard plots (Figure 8). Using the Ligand program, the best fit was for a five-parameter model with two specific sites and one nonspecific component (Table 3). Aldosterone binds with high affinity to a site that displays the properties of MR (K_d1 0.6 nM, N_{max}1 20 fmol/mg protein) and to a site with the

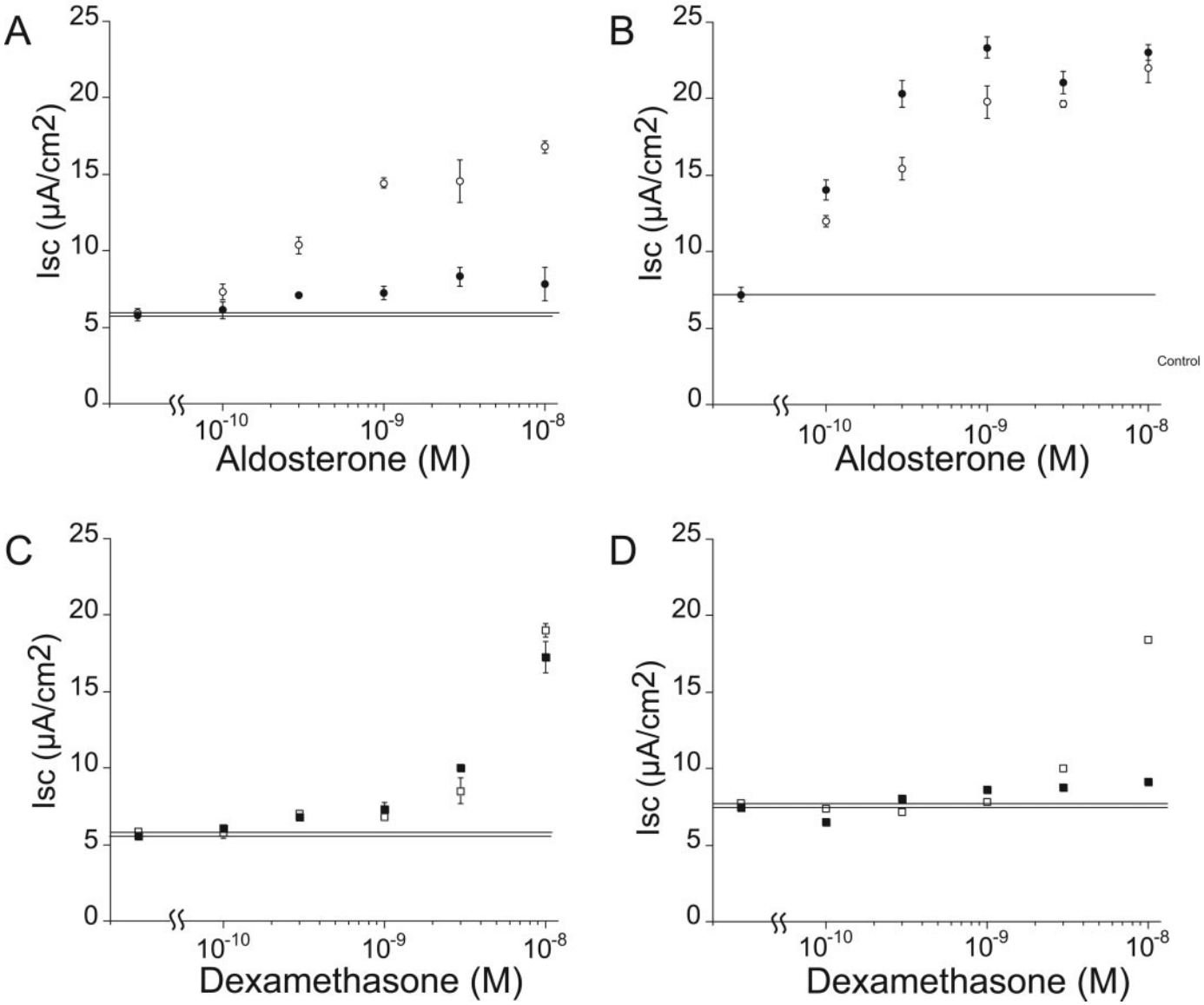

Figure 7. Mineralo- and glucocorticoid specificity of the sodium transport response. (A) Aldo (○), Aldo + Spiro 100× (●) 3 h. (B) Aldo (○), Aldo + RU486 100× (●) 3 h. (C) Dex (□) *versus* Dex + Spiro 100× (■) 3 h. (D) Dex (□) *versus* Dex + RU 486 100× (■) 3 h.

properties of GR (K_d2 85 nM, N_{max}2 310 fmol/mg protein). The binding sites for corticosterone were very similar to those of aldosterone for MR (K_d1 approximately 0.6 nM, N_{max}1 approximately 20 fmol/mg protein), with a higher affinity for GR but a similar number of receptors (K_d2 approximately 14 nM, N_{max}2 approximately 220 fmol/mg protein). Dexamethasone binds to a single class of binding sites (K_d approximately 9.7 nM) and a number of sites corresponding to the number of GR determined by corticosterone binding (N_{max} approximately 300 fmol/mg protein). As shown in Table 3, the properties of aldosterone binding in $mCCD_{cl1}$ cells that were grown on permeable supports are similar to those described above.

Discussion

A variety of *ex vivo* and *in vitro* models derived from *Xenopus* kidney (A6 cell line), toad urinary bladder, rat cortical collecting duct (RCCD cell lines), mouse kidney (M1), and mouse collecting duct (mpkCCDc14) (19–25) have been used to determine the effects of corticosteroids on sodium transport in tight epithelia. However, these studies were hampered by the fact that most of these cell systems do not express significant levels of functionally active MR and most of the described effects can be ascribed only to occupancy of the GR.

The mCCD clonal cell line ($mCCD_{cl1}$) that we report here has some novel and interesting features that made it ideally suitable for the aim of the present study. Between passages 19 and 35, the cells became more responsive to aldosterone and the dose-response curve became biphasic, indicating two $K_{1/2}$, one at approximately 0.5 nM and the other one at approximately 90 nM. The sodium currents (reaching up to 100 μAmp/cm^2 under maximal aldosterone stimulation) are completely inhibited by amiloride (Figure 1B), and, in fact, amiloride induced a reversal of the short-circuit current that is mediated by potassium secreted into

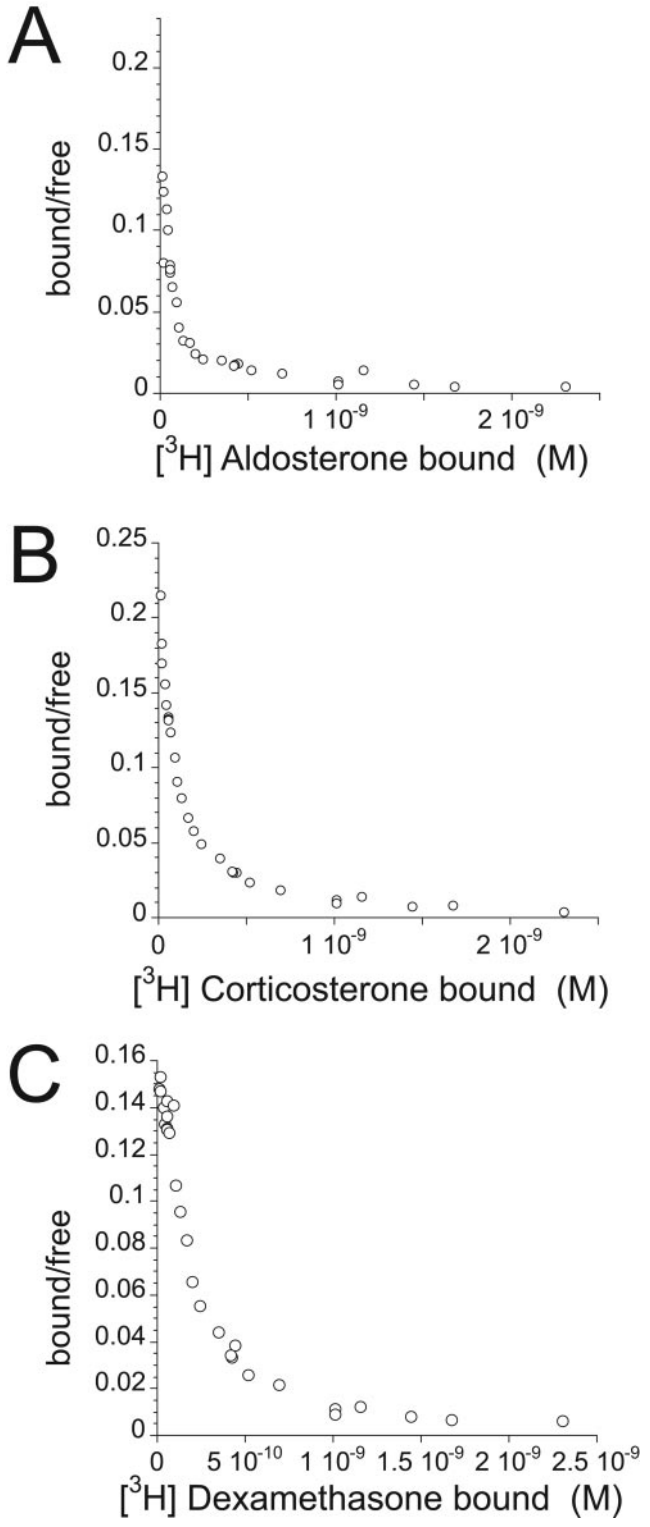

Figure 8. Equilibrium binding assay for aldosterone, corticosterone, and dexamethasone. Binding assay was performed on a cytoplasmic fraction of $mCCD_{cl1}$ cells that were grown on plastic Petri dishes as described in the Materials and Methods section. The data are displayed as Scatchard plots. *y* axis, bound/free hormone; *x* axis, bound hormone. The statistical analysis was performed according to the Ligand program, and the results are shown in Table 3. (A) Aldosterone. (B) Corticosterone. (C) Dexamethasone.

the apical medium (26). As shown here, the $mCCD_{cl1}$ cells express both MR and GR, which can be quantified by binding equilibrium assays, therefore allowing the correlation between MR and GR occupancy *versus* the sodium transport response.

Mineralocorticoid Specificity

The main working hypothesis to explain aldosterone specificity of binding and action in target cells such as kidney, toad bladder, and colon *in vivo*, in the presence of 100- to 1000-fold molar excess of circulating glucocorticoid, proposes that the 11β-HSD2 enzyme protects MR from exposure to glucocorticoid by rapidly converting cortisol (or corticosterone in rodents) into cortisone (or 11β-dihydroxy-corticosterone), their respective inactive metabolites (27). From this point of view, the A6 kidney cell is not an appropriate model for the mammalian kidney, because there is no evidence for expression of an active 11β-HSD2 enzyme in the cell line, suggesting that MR might be protected by other mechanisms, *in vitro* or *in vivo* (28). The TBM cell line responds equally well to aldosterone and corticosterone, indicating that endogenous 11β-HSD2 is expressed at low level in TBM cells (29). To our knowledge, the presence of 11β-HSD2 in M1 cells or rCCD2 has not been described. mpkCCD cells, however, do express 11β-HSD2 activity, albeit at a lower level than $mCCD_{cl1}$ cells, as shown by a transient sodium transport response upon corticosterone stimulation (30). The early phase of the sodium transport response, however, was indistinguishable from the aldosterone response, suggesting that the capacity (V_{max}) of the endogenous enzyme was not sufficient to metabolize corticosterone rapidly enough. The $mCCD_{cl1}$ cell line seems to display a higher activity of 11β-HSD2, because no sodium transport response is observed with concentrations of corticosterone up to 100 nM. By contrast, in the presence of carbenoxolone, which inhibits 11β-HSD2, the sodium transport is restored and displays the same pattern and affinity as for aldosterone. It is interesting that dexamethasone response (at low concentrations) was restored in the presence of carbenoxolone, suggesting that dexamethasone was converted into its 11-keto metabolite. 11-Keto-dexamethasone was shown recently to bind to GR with a comparable affinity (31) and very low affinity to MR. Transactivation of MR by dexamethasone or 11-keto-dexamethasone was weak or undetectable (31). 11β-HSD2 protected MR and GR from illicit occupation by cortisol but is unable to prevent activation of GR by 11-keto-dexamethasone. This provides more evidence for GR-mediated sodium transport.

Occupancy of GR and MR versus *Sodium Transport Response: Physiologic and Pathophysiologic Implications*

The cell line developed here is ideal to establish a quantitative relationship between MR and GR occupancy and the sodium transport response to various mineralocorticoid and glucocorticoid agonists.

Early Phase of Aldosterone Action: Implications in the Circadian Regulation of Sodium and Water Balance. Our data demonstrate clearly that the early phase of aldosterone action can be fully induced by low concentrations of aldosterone (between 30 pM and 1 nM, $K_{1/2}$ approximately 0.5 nM).

Table 3. Binding kinetics of (^{3}H)aldosterone, (^{3}H)corticosterone, and (^{3}H) dexamethasone on cytosol from $mCCD_{cl1}$ grown on plastic Petri dishes or Transwell filter cups

	Filter Cup	Plastic Petri Dishes		
	Aldosterone	Aldosterone	Corticosterone	Dexamethasone
Kd_1 (nM)	0.5	0.6	0.6	9.7
Kd_2 (nM)	90	85	14	
N_{1max} (fmol/mg protein)	23	19	19	300
N_{2max} (fmol/mg protein)	470	310	220	
Nonspecific ($M \times 10^{-3}$)	none	1.75	3.67	4.3
Best fit two- *versus* one-site model	$P < 0.001$	$P < 0.001$	$P < 0.001$	$P = 0.208$

This early response peaks at approximately 3 h and represents 20 to 35% of the maximal response observed under maximal hormonal concentration. It is interesting that this early response is transient, and, after 12 h, the sodium transport response tends to go back to control level. This seems not to be related to aldosterone metabolism in the target cell because addition of fresh hormone at 24 h was unable to elicit a significant sodium transport response (data not shown). The early phase of aldosterone action can be accounted for mainly by the occupancy of MR; the 200-fold difference in K_d between MR and GR does not prevent some overlap of binding, and, at any given aldosterone concentration, it is expected that some GR will be occupied (between 0.5 and 2%). It is not yet possible to say what is the physiologic importance of this binding; we provide here, however, pharmacologic evidence that the early phase of the physiologic response observed at low aldosterone concentration is fully blocked by spironolactone but not by the glucocorticoid antagonist RU486. It is interesting that a low dose of dexamethasone does not induce a sodium transport response comparable to that of aldosterone. By contrast, a high glucocorticoid concentration leads to an early and late effect, which is well maintained over 24 h of incubation. These observations have an implication in the circadian regulation of sodium and water balance. In humans (32) and rodents (33,34), plasma cortisol (corticosterone) and plasma aldosterone vary according to a circadian rhythm. Circadian rhythm of adrenal secretion of aldosterone and cortisol (or corticosterone in rodents) mediating sodium reabsorption in kidney and colon is maintained, independent of salt intake and activity (35), to adjust day and night the sodium balance. If the *in vitro* data obtained in the present study can be extrapolated to *in vivo*, then it is possible to predict the occupancy of MR and GR according to the hormonal profiles that have been published for rat or mice (Figure 9). The rapid and reversible action of aldosterone on ENaC activity is made possible by the rapid regulation of ENaC trafficking, achieved by posttranslational mechanisms implicating Sgk1 and Nedd4–2.

Long-Term Regulation under Chronic Salt Restriction. Plasma aldosterone has been reported to raise to high values in rats (36,37) under chronic salt restriction or in salt-losing mice (38). Under these circumstances, the plasma corticosterone is normal or slightly elevated. According to our model, the MR would be occupied approximately 95% and GR up to approximately 60% by aldosterone. This dual occupancy is expected to mediate the late phase of aldosterone action on sodium transport, which will be maintained as long as high concentrations of aldosterone would be maintained. Corticosterone under these circumstances will still be fully metabolized by 11β-HSD2 and thus plays little role in sodium balance. Dexamethasone, as well as its 11-keto metabolite, which binds preferentially to GR, can also elicit the sodium transport. At 10 nM dexamethasone, 50% of GR would be occupied, close to the EC50 for the sodium transport observed at 24 h.

Acute Regulation under Stress. Under stress, the situation may be different, and free cortisol (or corticosterone) may reach a level (up to 150 nM) that may well overcome the capacity of 11β-HSD2 (39,40). If we assume that free corticosterone in rodents will vary within the same range, then the 11β-HSD2 capacity may very well be surpassed and corticosterone will begin to occupy a significant proportion of MR and GR, contributing to the rapid regulation of all genes under the control of MR and GR.

Finally, our data suggest that the regulation of the transcriptome in the principal cell should now be investigated in a time- and dose-dependent manner to define the gene network that is more specifically linked to MR occupancy *versus* that which is related to occupancy of MR and GR by aldosterone and/or corticosterone. Until now, no hormonal regulatory elements specific to MR but only elements specific to GR have been identified in the promoter of induced or repressed genes. Mineralocorticoid specificity therefore is achieved by different mechanisms: At the prereceptor level (11β-HDSD2), at the receptor level, and at the level of transcription activation or repression (cell specific co-factor) (27). These molecular mechanisms are difficult to study *in vivo* because of the great heterogeneity of the kidney. Our clonal cell line should provide a tool first to identify *in vitro* the basic mechanisms of the transcriptional machinery of the principal cell.

Acknowledgments

This work was supported by the Swiss National Fund for Scientific Research, grant 3100-061966.00/1 (to B.C.R.), and the Botnar Foundation (to E.G.).

We thank E. Féraille for generous gift of a β Na,K-ATPase antiserum. We thank N. Skarda-Coderey for secretarial work. We thank D. Pearce for comments and suggestions.

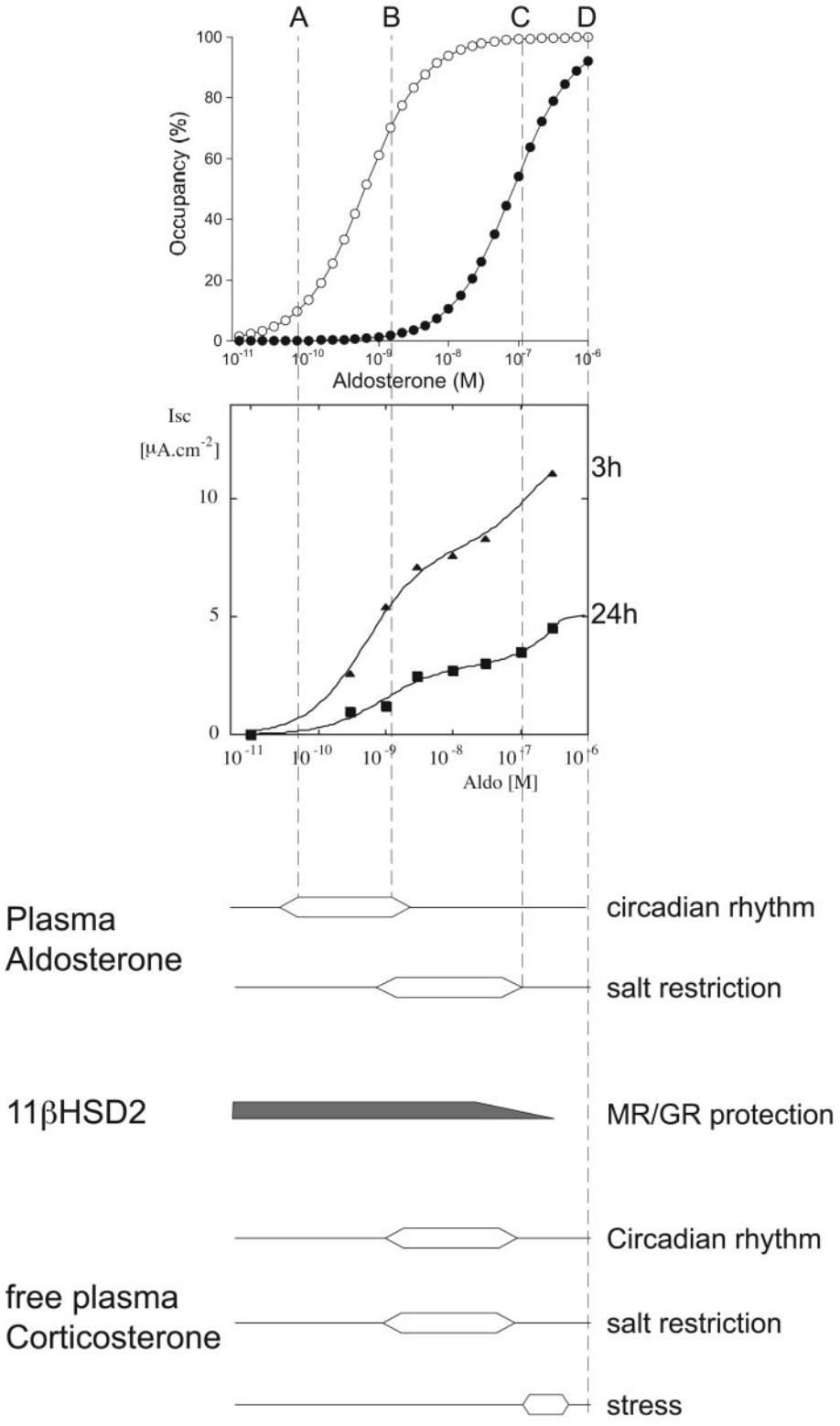

Figure 9. Correlation of MR and GR occupancy and early *versus* late sodium transport. Correlation between occupancy of MR *versus* GR by various agonists and the sodium transport responses I_{sc}. (Top) The relative receptor occupancy (% of maximum binding) of MR (○) and GR (●) was computed according to the parameters shown in Table 3 and is shown on the *y* axis as a function of aldosterone concentration (*x* axis). (Bottom) Sodium transport as measured by I_{sc} (*y* axis) as a function of aldosterone concentration (*x* axis). The dose-response curves measured at 3 h (▲) and at 24 h (■) are shown. Plasma aldosterone concentration and free plasma cortisol/corticosterone (see references in the Discussion section) during circadian rhythm, salt restriction, and stress are indicated to predict receptor occupancy (dashed vertical lines) at different hormonal concentrations. The degree of MR/GR protection by 11β-HSD2 is indicated, according to the *in vitro* data of the present study.

References

1. Verrey F, Hummler E, Schild L, Rossier BC: Control of sodium transport by aldosterone. In: *The Kidney, Physiology and Physiopathology*, edited by Giebisch G, Seldin D, Philadelphia, Lippincott Williams & Wilkins, 2000, pp 1441–1471
2. Horisberger JD, Diezi J: Effects of aldosterone on urinary excretion of lithium in the adrenalectomized rat. *Kidney Int* 20: 139, 1981
3. Horisberger JD, Diezi J: Inhibition of aldosterone effect on Na and K excretion by actinomycin D. *Kidney Int* 21: 904, 1982
4. Rossier BC, Geering K, Atkinson J, Roch-Ramel F: *Renal Receptors.* New York, Raven Press, pp 775–806 1985
5. Claire M, Rafestin-Oblin ME, Michaud A, Corvol P, Venot A, Roth-Meyer C, Boisvieux C, Mallet A: Statistical test of models and computerized parameter estimation for aldosterone binding in rat kidney. *FEBS Lett* 88: 295–299, 1978
6. Fagart J, Wurtz JM, Souque A, Hellal-Levy C, Moras D, Rafestin-Oblin ME: Antagonism in the human mineralocorticoid receptor. *EMBO J* 17: 3317–3325, 1998
7. Hellal-Levy C, Couette B, Fagart J, Souque A, Gomez-Sanchez C, Rafestin-Oblin ME: Specific hydroxylations determine selective corticosteroid recognition by human glucocorticoid and mineralocorticoid receptor. *FEBS Lett* 464: 9–13, 1999
8. Geering K, Claire M, Gaeggeler HP, Rossier BC: Receptor occupancy vs induction of Na-K-ATPase and Na+ transport by aldosterone. *Am J Physiol* 248: C102–C108, 1985
9. Edwards CRW: Renal 11-beta-hydroxysteroid dehydrogenase: A mechanism ensuring mineralocorticoid specificity. *Horm Res* 34: 114–117, 1990
10. Funder JW: Mineralocorticoids, glucocorticoids, receptors and response elements. *Science* 259: 1132–1133, 1993
11. Pradervand S, Wang Q, Burnier M, Beermann F, Horisberger JD, Hummler E, Rossier BC: A mouse model for Liddle's syndrome. *J Am Soc Nephrol* 10: 2527–2533, 1999
12. Pradervand S, Vandewalle A, Bens M, Gautschi I, Loffing J, Hummler E, Schild L, Rossier BC: Dysfunction of the epithelial sodium channel expressed in the kidney of a mouse model for Liddle syndrome. *J Am Soc Nephrol* 14: 2219–2228, 2003
13. Bens M, Van Huyen JP, Cluzeaud F, Teulon J, Vandewalle A: CFTR disruption impairs cAMP-dependent Cl(-) secretion in primary cultures of mouse cortical collecting ducts. *Am J Physiol* 281: F434–F442, 2001
14. Claire M, Steimer JL, Oblin ME, Gaeggeler HP, Venot A, Corvol P, Rossier BC: Cytoplasmic and nuclear uptake of aldosterone in toad bladder: A mathematical modeling approach. *Am J Physiol* 248: C88–C101, 1985
15. Loffing J, Moyer BD, McCoy D, Stanton BA: Exocytosis is not involved in activation of Cl-secretion via CFTR in Calu-3 airway epithelial cells. *Am J Physiol* 280: C913–C921, 1998
16. Rubera I, Loffing J, Palmer LG, Frindt G, Fowler-Jaeger N, Sauter D, Carroll T, McMahon A, Hummler E, Rossier BC: Collecting duct-specific gene inactivation of alphaENaC in the mouse kidney does not impair sodium and potassium balance. *J Clin Invest* 112: 554–565, 2003
17. Féraille E, Carranza ML, Gonin S, Béguin P, Pedemonte CH, Rousselot M, Caverzasio J, Geering K, Martin PY, Favre H: Insulin-induced stimulation of Na+,K+ ATPase activity in kidney proximal tubule cells depends on phosphorylation of the alpha-subunit at Tyr-10. *Mol Biol Cell* 10: 2847–2859, 1999
18. Horisberger JD, Diezi J: Inhibition of aldosterone-induced antinatriuresis and kaliuresis by actinomycin D. *Am J Physiol* 246: F201–F204, 1984
19. Handler JS, Steele RE, Sahib MK, Wade JB, Preston AS, Lawson NL, Johnson JP: Toad urinary bladder epithelial cells in culture: Maintenance of epithelial structure, sodium transport, and response to hormones. *Proc Natl Acad Sci U S A* 76: 4151–4155, 1979
20. Claire M, Machard B, Lombès M, Oblin ME, Bonvalet JP, Farman N: Aldosterone receptors in A6 cells: Physicochemical characterization and autoradiographic study. *Am J Physiol* 257: C665–C677, 1989
21. Chen SY, Wang J, Liu WH, Pearce D: Aldosterone responsiveness of A6 cells is restored by cloned rat mineralocorticoid receptor. *Am J Physiol* 43: C39–C46, 1998
22. Blot-Chabaud M, Laplace M, Cluzeaud F, Capurro C, Cassingena R, Vandewalle A, Farman N, Bonvalet JP: Characteristics of a rat collecting duct cell line that maintains high transepithelial resistance. *Kidney Int* 50: 367–376, 1996
23. Djelidi S, Beggah A, Courtois-Coutry N, Fay M, Cluzeaud F, Viengchareun S, Bonvalet JP, Blot-Chabaud M: Basolateral translocation by vasopressin of the aldosterone-induced pool of latent Na-K-ATPases is accompanied by alpha1 subunit dephosphorylation: Study in a new aldosterone-sensitive rat cortical collecting duct cell line. *J Am Soc Nephrol* 12: 1805–1818, 2001
24. Le Moellic C, Ouvrard-Pascaud A, Capurro C, Cluzeaud F, Fay M, Jaisser F, Farman N, Blot-Chabaud M: Early nongenomic events in aldosterone action in renal collecting duct cells: PKC alpha activation, mineralocorticoid receptor phosphorylation and cross-talk with the genomic response. *J Am Soc Nephrol* 15: 1145–1160, 2004
25. Stoos BA, Naray-Fejes-Toth A, Carretero OA, Ito S, Fejes-Toth G: Characterization of a mouse cortical collecting duct cell line. *Kidney Int* 39: 1168–1175, 1991
26. Horisberger JD, Guisan B, Gaeggeler HP, Rossier BC: Regulation of K+ secretion in a novel cortical collecting duct mouse cell line [Abstract]. *J Am Soc Nephrol* 2004, in press LG: Epithelial Na channels and short-term renal response to salt deprivation. *Am J Physiol* 283: F717–F726, 2002
27. Farman N, Rafestin-Oblin ME: Multiple aspects of mineralocorticoid selectivity. *Am J Physiol* 280: F181–F192, 2001
28. Morris DJ, Latif SA, Rokaw MD, Watlington CO, Johnson JP: A second enzyme protecting mineralocorticoid receptors from glucocorticoid occupancy. *Am J Physiol* 43: C1245–C1252, 1998
29. Duperrex H, Kenouch S, Gaeggeler HP, Seckl JR, Edwards CRW, Farman N, Rossier BC: Rat liver 11beta-hydroxysteroid dehydrogenase complementary deoxyribonucleic acid encodes oxoreductase activity in a mineralocorticoid-responsive toad bladder cell line. *Endocrinology* 132: 612–619, 1993
30. Bens M, Vallet V, Cluzeaud F, Pascual-Letallec L, Kahn A, Rafestin-Oblin ME, Rossier BC, Vandewalle A: Corticosteroid-dependent sodium transport in a novel immortalized mouse collecting duct principal cell line. *J Am Soc Nephrol* 10: 923–934, 1999

31. Rebuffat AG, Tam S, Nawrocki AR, Baker ME, Frey FJ, Odermatt O: The 11-keto-steroid 11-keto-dexamethasone is a glucocorticoid receptor agonist. *Mol Cell Endocrinol* 214: 27–37, 2004
32. Hurwitz S, Cohen RJ, Williams GH: Diurnal variation of aldosterone and plasma renin activity: Timing relation to melatonin and cortisol and consistency after prolonged bed rest. *J Appl Physiol* 96: 1406–1414, 2004
33. Hilfenhaus M: Circadian rhythm of the renin-angiotensin-aldosterone system in the rat. *Arch Toxicol* 36: 305–316, 1976
34. Le Minh N, Damiola F, Tronche F, Schutz G, Schibler U: Glucocorticoid hormones inhibit food-induced phase-lifting of peripheral circadian oscillators. *EMBO J* 20: 7128–7136, 2001
35. Wang Q, Horisberger JD, Maillard M, Brunner HR, Rossier BC, Burnier M: Salt- and angiotensin II-dependent variations in amiloride-sensitive rectal potential difference in mice. *Clin Exp Pharmacol Physiol* 27: 60–66, 2000
36. Pacha J, Frindt G, Antonian L, Silver RB, Palmer LG: Regulation of Na channels of the rat cortical collecting tubule by aldosterone. *J Gen Physiol* 102: 25–42, 1993
37. Gomez-Sanchez EP, Ahmad N, Romero DG, Gomez-Sanchez CE: Origin of aldosterone in the rat heart. *Endocrinology* 145: 4796–4802, 2004
38. Wang Q, Clement S, Gabbiani G, Horisberger JD, Burnier M, Rossier BC, Hummler E: Chronic hyperaldosteronism in a transgenic mouse model fails to induce cardiac remodeling and fibrosis under a normal-salt diet. *Am J Physiol* F1178–F1184, 2004
39. Vogeser M, Briegel J, Zachoval R: Dialyzable free cortisol after stimulation with Synachten. *Clin Biochem* 35: 539–543, 2002
40. Vogeser M, Groetzner J, Kupper C, Briegel J: Free serum cortisol during postoperative acute response determined by equilibrium dialysis and liquid chromatography-tandem mass spectrometry. *Clin Chem Lab Med* 41: 146–151, 2003